Vibration measurement by use of wavelet transform and temporal carrier technique

C Quan, Y Fu and C J Tay

Department of Mechanical Engineering, National University of Singapore, 10 Kent Ridge Crescent, Singapore 119260, Singapore

E-mail: mpeqcg@nus.edu.sg

Abstract

In this paper, two optical techniques, namely, electronic speckle pattern interferometry (ESPI) and fringe projection, are described for the measurement of a low-frequency vibrating object. The combination of optical interferometry and temporal phase analysis allows the measurement on a continuously deforming object without the spatial phase unwrapping process. A series of speckle or fringe patterns is captured by a high-speed CCD camera, and the intensity variation of each pixel on the recorded images is analysed along the time axis using the temporal wavelet transform method that has the property of adaptive band-pass filtering of a measured signal. However, the wavelet transform method is unable to determine the sign of a phase and it is difficult to analyse a part of the object that is not moving. The sign ambiguity problem can be overcome by adding a temporal carrier in the image acquisition process. In the ESPI, a temporal carrier is introduced by a PZT stage in the reference beam of the interferometer. In the fringe projection technique, a laterally shifted fringe pattern is projected on a vibrating object. After the temporal carrier is removed, the absolute displacement of a vibrating object is obtained without the need for a temporal or spatial phase unwrapping process.

Keywords: vibration measurement, wavelet transform, temporal carrier, electronic speckle pattern interferometry (ESPI), fringe projection

1. Introduction

In deformation measurement, the study of the response of objects to impact loading or vibration is a subject of great interest in experimental mechanics and constitutes one of the most appealing applications of optical interferometry. High resolution 3D displacement or surface profiling of a vibrating object or an object with a continuous changing profile can provide useful information on the dynamic response and deformation of the object. However, this information would be difficult to obtain using the phase shifting technique [1] or time averaged methods. Due to the rapid development of a high-speed digital recording device, it is now possible to record speckle or fringe patterns with rates exceeding 100 000 frames per second (fps). For example, the Photron ultima APX high-speed camera has a capturing rate up to 120 000 fps. Retrieving precise instantaneous spatial phase maps from those speckle or fringe patterns along the time axis enables an instantaneous 3D profile and deformation as well as dynamic response to be studied. Generally, two methods are used to analyse the instantaneous fringe patterns, namely, spatial phase analysis and temporal phase analysis. The spatial phase analysis is a technique to retrieve an instantaneous phase map from one

fringe pattern [2]. In the late 1990s, a new phase evaluation technique based on temporal analysis was introduced [3–5]. In this technique, a sequence of fringe patterns is recorded throughout the entire deformation history of the object. Each pixel is then analysed as a function of time. The phase of the fringe patterns is related to different physical parameters depending on the optical arrangements. In recent years, continuous wavelet transform (CWT) has been applied to the temporal phase analysis of speckle interferometry. The concept was first introduced by Colonna de Lega in 1996, and some preliminary results were presented [6]. Our previous results also showed the advantages of the wavelet transform compared with the Fourier transform in the temporal phase analysis [7–9]. As the wavelet analysis calculates the frequency with maximum energy at each instant, it performs an adaptive band-pass filtering of the measured signal, thus limiting the influence of various noise sources and increasing the measurement resolution significantly.

The temporal phase analysis technique has the advantage of eliminating speckle noise, as it evaluates the phase pixel by pixel along the time axis. However, it does have its disadvantage: it cannot analyse part of an object that is not moving with the rest nor objects that deform in opposite directions at different parts. Determination of an absolute sign of the phase change is impossible by both temporal Fourier and wavelet analyses. This limits the technique to the measurement of deformation in one direction which is already known. Adding a carrier frequency to the image acquisition process is a method to overcome these problems. In this study, a temporal carrier is applied with ESPI and fringe projection techniques. The phase is retrieved by temporal wavelet transform. The phase variation due to the temporal carrier is also measured experimentally. After removing the effect of the temporal carrier, the absolute phase change is obtained.

2. Theoretical analysis

2.1. Wavelet phase extraction

Wavelet analysis has become an effective tool in many research areas since the last decade. An interesting historical account by Daubechies [10] shows that different domains of physics and engineering have developed methods that can all be brought into a larger perspective based on wavelets. The same situation applies in optical metrology.

Wavelet transform maps a signal $s(t)$ into a two-dimensional domain (the time–frequency plane) and is denoted by

$$W_S(a,b) = \frac{1}{\sqrt{a}} \int_{-\infty}^{+\infty} s(t) \Psi \left(\frac{t-b}{a} \right) \mathrm{d}t = \int_{-\infty}^{+\infty} s(t) \bar{\Psi}_{ab}(t)\, \mathrm{d}t, \tag{1}$$

where $\Psi(t)$ is in general called the mother wavelet, and the basis functions of the transform, called the daughter wavelets, are given by

$$\Psi_{ab}(t) = \frac{1}{\sqrt{a}} \Psi \left(\frac{t-b}{a} \right). \tag{2}$$

Ψ_{ab} is a set of basis functions obtained from the mother wavelet $\Psi(t)$ by compression or dilation

using a scaling parameter a and temporal translation using a shift parameter b. $\overline{\Psi}_{ab}$ denotes the complex conjugate of Ψ_{ab}.

In the application of phase extraction from a one-dimensional signal, the complex Morlet wavelet is selected as a mother wavelet because it gives the smallest Heisenberg box:

$$\psi(t) = \exp(-t^2/2)\exp(\mathrm{i}\omega_0 t). \tag{3}$$

Here, the central frequency $\omega_0 = 2\pi$ is chosen to satisfy the admissibility condition [11]. CWT expands a one-dimensional temporal intensity variation of certain pixels into a two-dimensional plane of the scaling factor a (which is related to the frequency) and position b (which is the time axis). The trajectory of maximum $\left|W_{xy}(a,b)\right|^2$ on the a–b plane is called a 'ridge'. The instantaneous frequency of the signal $\varphi'_{xy}(b)$ is calculated as

$$\varphi'_{xy}(b) = \frac{\omega_0}{a_{rb}}, \tag{4}$$

where a_{rb} denotes the value of a at instant b on the ridge. The phase change $\Delta\varphi_{xy}(t)$ can be calculated by integration of the instantaneous frequency in equation (4), so that the phase unwrapping procedure is not needed in temporal and spatial domains. Subtracting the phase change due to the temporal carrier, the absolute phase change representing different physical quantities can be obtained on each pixel.

2.2. Electronic speckle pattern interferometry

Electronic speckle pattern interferometry (ESPI) involves recording two speckle patterns of an object corresponding to two slightly different states. For an object having a diffuse surface, each speckle pattern is the result of two light wavefronts interfering at the image plane of a CCD camera. The light wavefronts are the reference wavefront, which is an expanded beam of a laser, and the object wavefront, which is scattered from the laser-illuminated object surface.

The intensity distribution is generally expressed in the following manner:

$$I = I_0 + I_M \cos\varphi, \tag{5}$$

where I_0 and I_M are the background and modulation intensity, respectively. φ is the phase value which is different for different deformed states. When the intensities of a reference state and deformed states are recorded, they can be described by

$$\begin{aligned} I_i &= I_0 + I_M \cos\varphi_i \\ I_d &= I_0 + I_M \cos(\varphi_i + \Delta\varphi), \end{aligned} \tag{6}$$

where $\Delta\varphi$ is the phase change due to deformation. Since φ_i is a random variable, neither image displays any fringe pattern. However if these two images are subtracted from each other, we can obtain

$$\Delta I = |I_d - I_i| = 2I_M \left|\sin\left(\varphi_i + \frac{\Delta\varphi}{2}\right)\sin\left(\frac{\Delta\varphi}{2}\right)\right|. \tag{7}$$

While the values of φ_i and I_M vary randomly from one point to another, the $\sin(\Delta\varphi/2)$ term is

generally a slowly varying modulation of the random intensity difference. Dark and bright areas show up as correlation fringes. Correlation by subtraction can be done electronically in real time, thus enabling visualization of the evolution of fringe patterns. ESPI can be used to measure in-plane and out-of-plane displacements depending on the optical arrangement.

2.3. Fringe projection for shape measurement

Fringe projection [12] is not an interferometric technique in essence, but it provides fringe patterns very similar to two wavefront interferograms. Hence, fringe analysis methods can be used to obtain quantitative information. In the fringe projection technique, a known fringe pattern, in our case a linear grating with sinusoidal wave configuration, is projected onto a surface of interest at a certain angle; the distribution of the fringe pattern on the surface is perturbed in accordance with the profile of a test surface when it is observed from a different angle. Thereby a three-dimensional feature of the object is converted into a two-dimensional image.

Figure 1 shows the schematic layout of the fringe projection and imaging system. With normal viewing, the phase change φ due to the height h_F is given by [13]

$$h_F = \frac{L_F}{d_F}\frac{\varphi}{2\pi f_0} = k_F\varphi, \tag{8}$$

where L_F is the distance between the fringe projector and the reference plane, d_F is the distance between the projector and camera axis, f_0 is the spatial frequency of the projected fringes on the reference plane and k_F, which can be obtained by calibration, is an optical coefficient related to the configuration of the system. φ is the phase angle change which contains information on the surface height information.

When a sinusoidal fringe pattern (i.e. straight lines parallel to the reference *y*-axis in figure 1) is projected onto an object, the mathematical representation of the intensity distribution captured by a CCD camera is governed by the following equation:

$$I(x, y) = I_0(x, y) + I_M(x, y)\cos[2\pi f_0 x + \varphi(x, y)], \tag{9}$$

where $I_0(x, y)$ and $I_M(x, y)$ are the background and modulation factor, respectively, and $\varphi(x, y)$ is the phase which contains the shape information.

The fringe projection technique has the following merits: (1) easy implementation; (2) phase shifting, fringe density and direction change can be realized with no moving parts if a computer controlled fringe projector is used and (3) fast full field measurement. Because of these advantages, the coordinate measurement and machine vision industries have started to commercialize the fringe projection method, and some encouraging applications have been reported by Gartner *et al* [14], Muller [15] and Sansoni *et al* [16].

3. Experimental setup

Figure 2 shows an ESPI setup which is similar to a Michelson interferometer for out-of-plane displacement measurement. A He–Ne laser beam (30 mW, $\lambda = 632.8$ nm) illuminates a specimen and a reference plate at right angles through a beam splitter. In the *z*-direction, the sensitivity or amount of deformation that produces one fringe is $\lambda/2$, where λ is the wavelength of the laser. The

setup is used for measurement of a vibrating test specimen with a temporal carrier. The test specimen is a perspex cantilever beam with a diffuse surface. It is subjected to a sinusoidal vibration at the free end using a vibrator. The frequency of vibration is controlled by a function generator and the area near the clamped end is measured. To generate a temporal carrier, a reference plate is mounted on a computer-controlled piezoelectric transducer. During vibration, the reference plate is given a linear rigid body motion with a certain velocity. In order to retrieve the phase change of the temporal carrier, a stationary reference block with a diffuse surface is mounted above the vibrating beam and its image is captured together with the vibrating beam.

The experimental setup for the fringe projection method is shown in figure 3. A grating mounted on a motorized stage is projected onto a vibrating object by an imaging lens, and the projected fringe pattern is captured using a high-speed camera with a telecentric lens. The temporal carrier is generated by shifting the grating on the motorized stage at a constant speed. The specimen measured is a cantilever beam similar to that used in the previous ESPI setup. It is also excited at one end, but with a larger vibrating amplitude to meet the sensitivity of the fringe projection technique.

4. Results and discussions

In ESPI experiment, a series of speckle pattern (512 pixel × 480 pixel) is captured by a high-speed camera (KODAK Motion Corder Analyzer, SR-Ultra) with an interval of 0.004 s and an imaging rate of 250 frames per second. The area of interest on the beam with a length and width of 60.8 mm and 15.2 mm, respectively, contains 400 pixels ×100 pixels. Five hundred speckle patterns were captured over a 2 s period, and 400 consecutive images were arbitrarily selected for processing. For each pixel, 400 sampling points along the time axis were obtained. Figure 4(a) shows the intensity variations of a point on the cantilever beam. Figure 4(b) shows the modulus of the Morlet wavelet transform. The dashed line shows the ridge of the wavelet transformation where the maximum modulus is obtained. Integration of $2\pi/a_{rb}$ was carried out along the time axis to generate a continuous phase change $\Delta\varphi(t)$. Figure 5(a) shows the temporal phase change obtained on the cantilever beam and reference block. The difference between these two lines gives the absolute phase change of that point due to vibration. In the speckle interferometer, as shown in figure 2, a 2π phase change represents a displacement of $\lambda/2$ (= 316.4 nm) in the z-direction. Figure 5(b) shows the temporal displacement obtained of the point. The spatial distribution of the displacement is obtained by the combination of the results for all the points.

In vibration measurement by the fringe projection technique, a theoretical temporal carrier is not necessary as the fringe patterns already contain a spatial carrier. The phase can be extracted spatially by the Fourier [17] or wavelet transform [18]. Figure 6(a) shows a typical fringe pattern on a vibrating cantilever beam and figure 6(b) shows a wrapped phase map after 2D Fourier transform. Spatial techniques require a complete matrix to be processed; however, in many cases some information is lost due to the shape, defect, height step or discontinuity of the objects. The cantilever beam shown in figure 6 has four through-holes. It can be observed that the phase distortion around the holes after phase unwrapping is obvious as there is no intensity variation within the holes (figure 6(c)).

In this case, a temporal carrier is introduced to overcome this problem. Instead of a fixed fringe pattern, a shifted fringe pattern is projected on the specimen. It is noteworthy that the temporal carrier frequency should not be too high due to the limitation of the Nyquist sampling theorem. Figure 7(a) shows the grey value variation at point A (shown in figure 6(a)) and the modulus of the Morlet wavelet transform (figure 7(b)). The pixels with little intensity variation can be masked

easily. Similar to the previous case in ESPI, the spatial distribution of displacement can be obtained by the combination of the results on valid pixels. Figure 8 shows the displacement maps at different instants.

5. Concluding remarks

This paper presents a novel method to retrieve the transient phase change on a vibrating object using the combination of temporal wavelet and temporal carrier. The introduction of a temporal carrier ensures that the phase change of each point on an object is in one direction, so that the temporal phase analysis can be applied. Subsequently, the temporal carrier is removed and the absolute displacement of a vibrating object is obtained. Two applications of the temporal carrier are illustrated with different optical techniques. It can be observed that in some cases the temporal phase extraction and temporal carrier technique are able to eliminate phase distortion due to irregularity of an object and exploit the advantages of one-dimensional temporal image processing.

References

[1] Huntley J M, Kaufmann G H and Kerr D 1999 Phase-shifted dynamic speckle pattern interferometry at 1 kHz *Appl. Opt.* **38** 6556

[2] Takeda M, Ina H and Kobayashi S 1982 Fourier-transform method of fringe-pattern analysis for computer-based topography and interferometry *J. Opt. Soc. Am.* **72** 156

[3] Tiziani H J 2000 Spectral and temporal phase evaluation for interferometry and speckle applications *Trends in Optical Nondestructive Testing and Inspection* ed P K Rastogi and D Inaudi (Amsterdam: Elsevier) p 323

[4] Huntley J M and Saldner H 1993 Temporal phase-unwrapping algorithm for automated interferogram analysis *Appl. Opt.* **32** 3047

[5] Kauffmann J and Tiziani H J 2006 Time resolved vibration measurement with temporal speckle pattern interferometry *Appl. Opt.* **45** 6682

[6] Colonna de Lega X 1996 Continuous deformation measurement using dynamic phase-shifting and wavelet transform *Applied Optics and Optoelectronics 1996* ed K T V Grattan (Bristol: Institute of Physics Publishing) p 261

[7] Fu Y, Tay C J, Quan C and Chen L J 2004 Temporal wavelet analysis for deformation and velocity measurement in speckle interferometry *Opt. Eng.* **43** 2780

[8] Tay C J, Quan C, Fu Y and Huang Y 2004 Instantaneous velocity displacement and contour measurement by use of shadow moire and temporal wavelet analysis *Appl. Opt.***43** 4164

[9] Fu Y, Tay C J, Quan C and Miao H 2005 Wavelet analysis of speckle patterns with a temporal carrier *Appl. Opt.***44** 959

[10] Daubechies I 1992 *Ten Lectures on Wavelets* (Philadelphia,PA: Society for Industrial and Applied Mathematics)

[11] Chui C K 1992 *An Introduction to Wavelets* (Boston, MA: Academic)

[12] Srinivasan V H, Liu C and Halioua M 1984 Automated phase measuring profilometry of 3D diffuse objects *Appl. Opt.* **23** 3105

[13] Quan C, He X Y, Tay C J and Shang H M 2000 3D surface profile measurement using LCD fringe projection *Proc. SPIE* **4317** 511

[14] Gartner H, Lehle P and Tiziani H J 1995 New, high efficient binary codes for structured light methods *Proc. SPIE* **2599** 4

[15] Muller E 1995 Fast three dimensional form measurement system *Opt. Eng.* **34** 2754

[16] Sansoni G, Corini S, Lazzari S, Rodella and Docchio F 1997 Three dimensional imaging based on gray-code light projection: characterization of the measuring algorithm and

development of a measuring system for industrial application *Appl. Opt.* **36** 4463

[17] Tay C J, Quan C, Shang H M, Wu T and Wang S H 2003 New method for measuring dynamic response of small components by fringe projection *Opt. Eng.* **42** 1716

[18] Federico A and Kaufmann G H 2002 Evaluation of the continuous wavelet transform method for phase measurement of electronic speckle pattern interferometry fringes *Opt. Eng.* **41** 3209

List of Figures

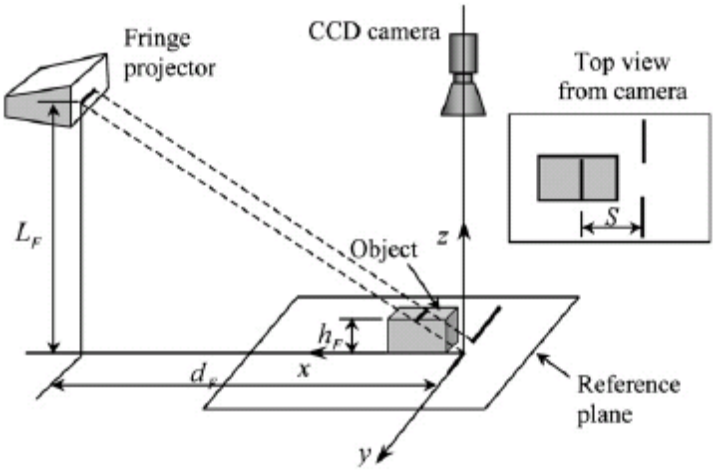
Fringe
projector
CCD camera
Top view
from camera
L_F
Object
z
S
h_F
d_F
x
Reference
plane
y

Fig. 1

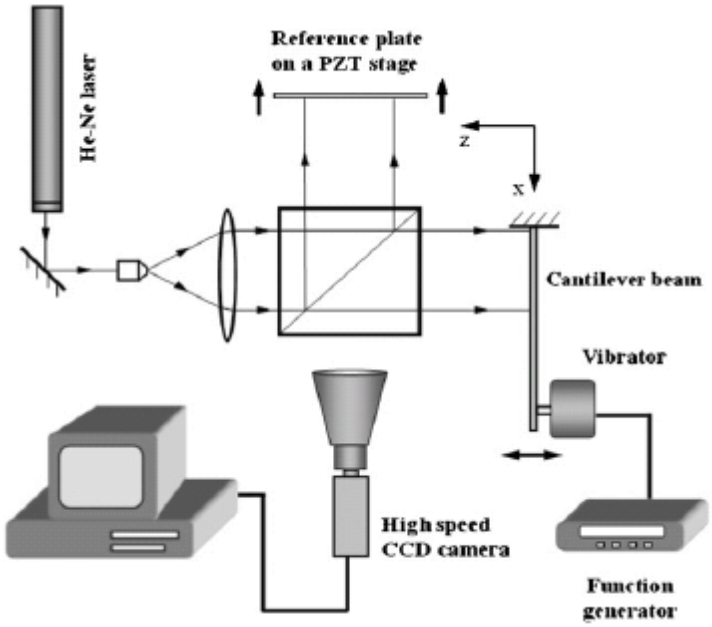
Reference plate
on a PZT stage
He-Ne laser
z
x
Cantilever beam
Vibrator
High speed
CCD camera
Function
generator

Fig. 2

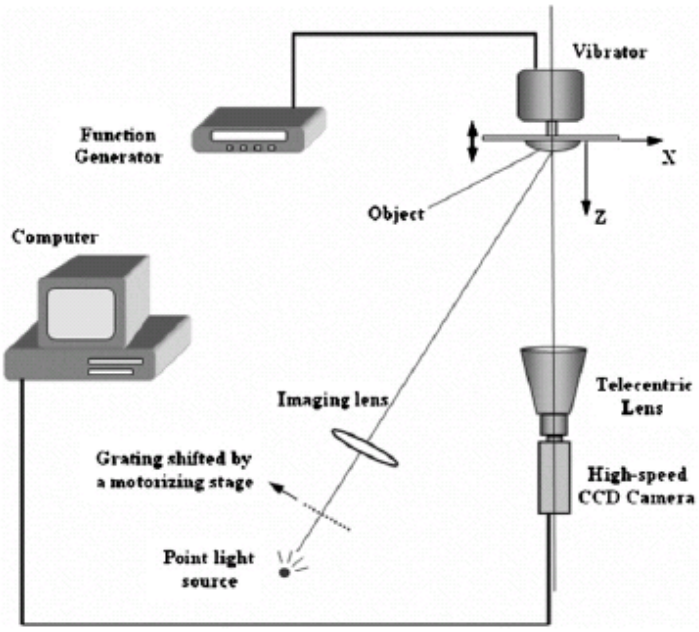
Vibrator
Function Generator
X
Z
Object
Computer
Imaging lens
Telecentric Lens
Grating shifted by a motorizing stage
High-speed CCD Camera
Point light source

Fig. 3

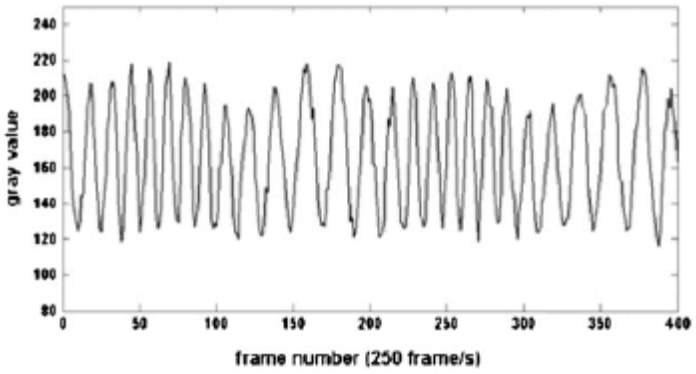
gray value
240
220
200
180
160
140
120
100
80
0
50
100
150
200
250
300
350
400
frame number (250 frame/s)

(*a*)

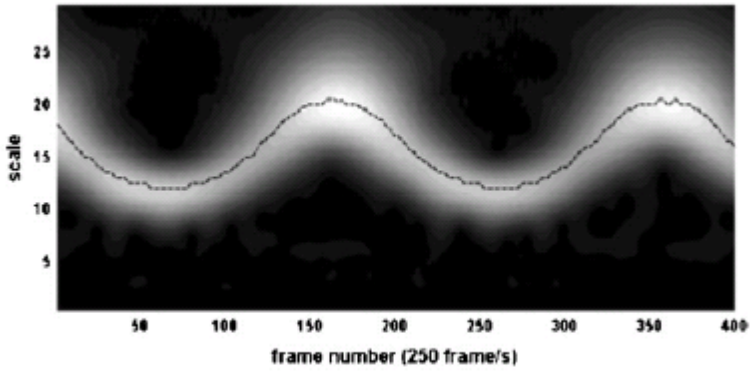
scale
25
20
15
10
5
50
100
150
200
250
300
350
400
frame number (250 frame/s)

(*b*)

Fig. 4

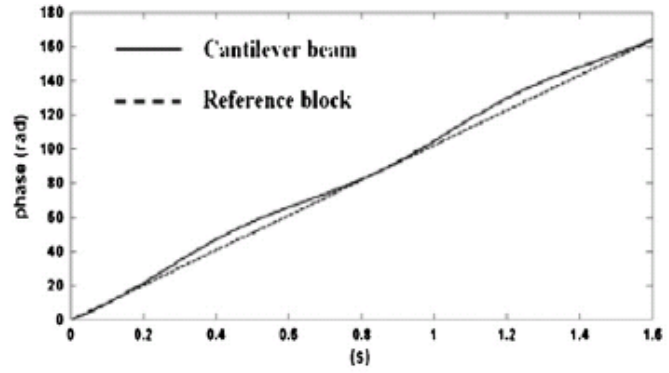
Cantilever beam
Reference block
phase (rad)
(s)

(*a*)

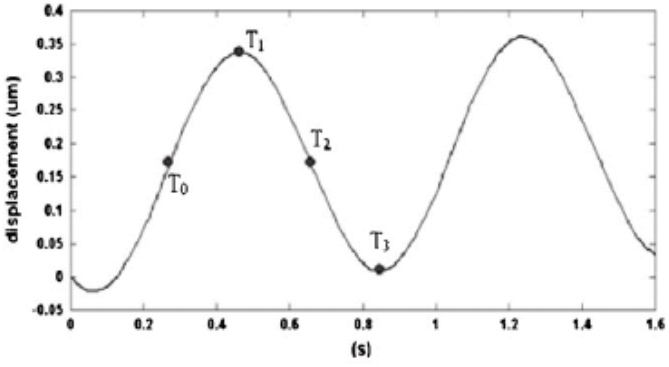
T1
T2
T0
T3
displacement (um)
(s)

(*b*)

Fig. 5

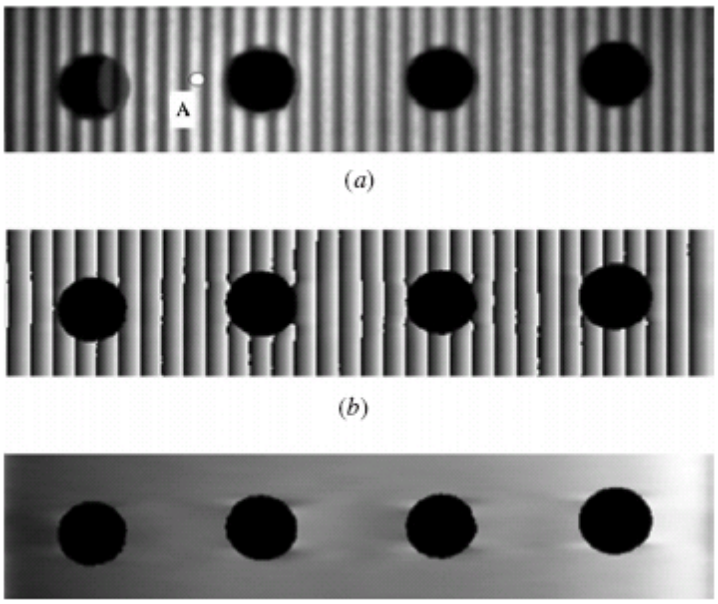

Fig. 6

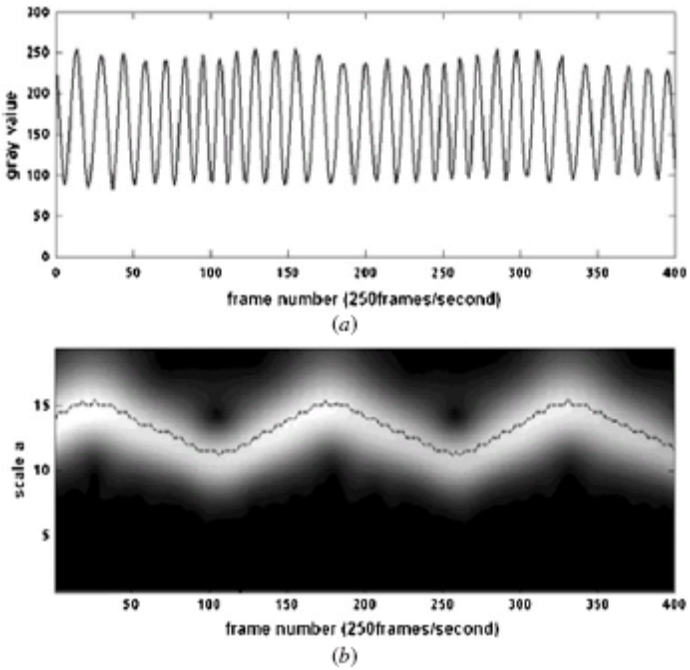
gray value
frame number (250frames/second)
(a)
scale a
frame number (250frames/second)
(b)

Fig. 7

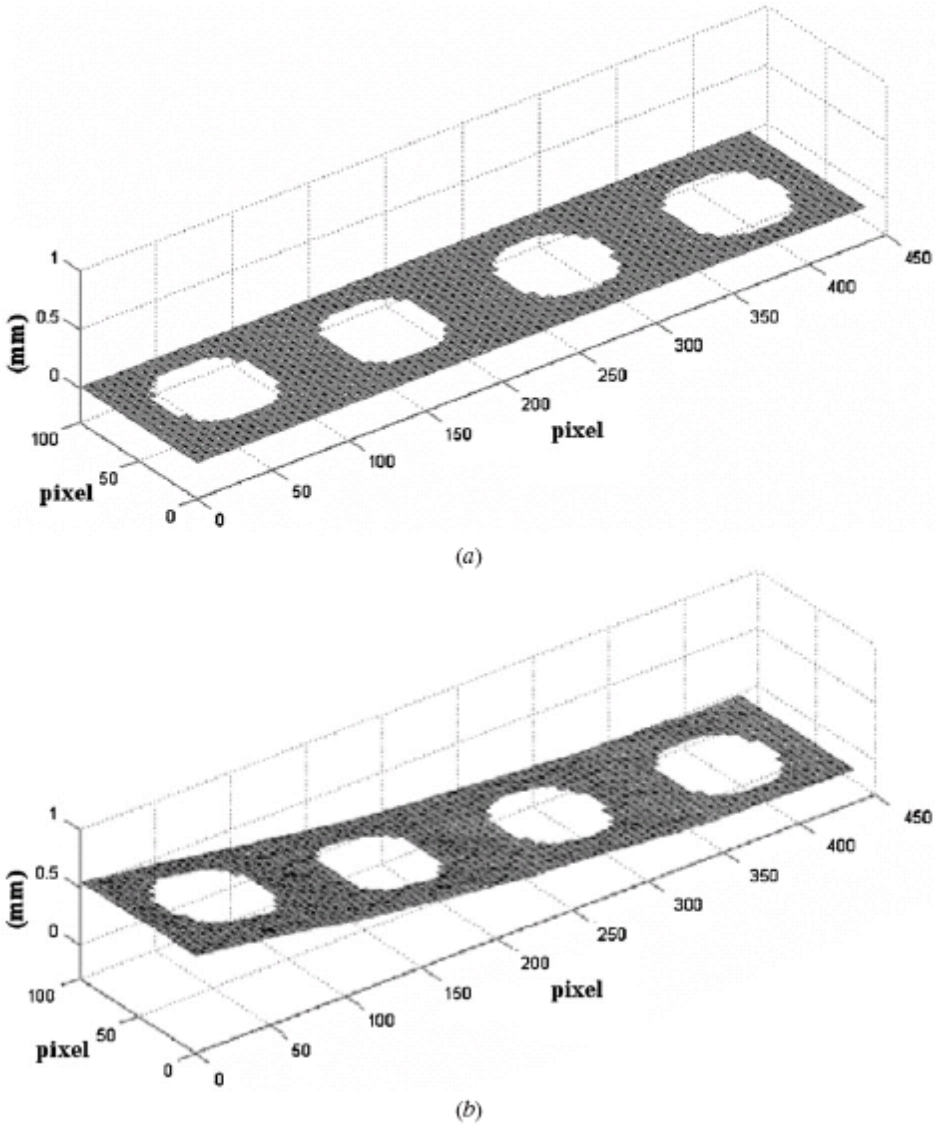

(*a*)

(*b*)

Fig. 8